Cyclosporine A effectively inhibits graft-versus-host disease during development of Epstein-Barr virus-infected human B cell lymphoma in SCID mouse

Runliang Gan,[1] Zhihua Yin,[2] Tengfei Liu,[2] Lijiang Wang,[1] Yunlian Tang[1] and Ying Song[1]

[1]Cancer Research Institute, Medical School, Nanhua University, Hengyang 421001, P. R. China; and [2]Key Lab of Carcinogenesis of Chinese Health Ministry, Hunan Medical University, Changsha 410078, P. R. China

(Received June 5, 2003/Revised July 10, 2003/Accepted July 10, 2003)

We previously constructed human peripheral blood lymphocyte (hu-PBL)/severe combined immunodeficiency mouse (SCID) chimeras and induced human B-cell lymphomas associated with Epstein-Barr virus (EBV) in SCID mice. However, a number of SCID mice died of graft-versus-host disease (GVHD) during the early experimental course. The aim of this study was to test the efficacy of cyclosporine A (CSA) for prevention of GVHD and to define how CSA inhibits the occurrence of GVHD and the production of soluble interleukin (IL) 2 receptor (sIL-2R) in hu-PBL/SCID mice. No mouse died in the active EBV infection group with CSA administration, while 17 mice in three groups without CSA administration died of GVHD. Mortalities in these three groups were 55.56% (5/9), 30.43% (7/23), and 27.78% (5/18), and the medium life span was 17 days. Over the first 33 days after hu-PBL transplantation, serum level of human sIL-2R in hu-PBL/SCID chimeras was stable in the active EBV infection plus CSA group, while sIL-2R concentration gradually increased in the sera of mice with active EBV infection without CSA administration and peaked at 22 days. Thirty-two mice developed tumors among the 43 surviving SCID mice. There was no significant difference of tumor incidence between the active EBV infection groups with CSA and without CSA administration ($P>0.05$). From their morphological and immunohistochemical features, as well as detection of human Alu-sequence and EBV in tumor cells, these EBV-induced tumors were identified as human B-cell lymphomas. Thus, CSA can strikingly inhibit GVHD in hu-PBL/SCID chimeras, and should therefore be effective to establish a stable SCID mouse model of human lymphoma associated with EBV. Treatment with CSA had no effect on the tumor incidence in hu-PBL/SCID chimeras after active EBV infection. Accordingly, serum level of sIL-2R is a valuable indicator of GVHD occurrence in hu-PBL/SCID chimeras. (Cancer Sci 2003; 94: 796–801)

Epstein-Barr virus (EBV) is designated as a γ herpesvirus. This ubiquitous transforming virus is known to infect both epithelial and lymphoid cells. More than 90% of the world population is seropositive for EBV. EBV has been shown to be related to a whole range of benign and malignant human diseases. EBV is an etiological agent of infectious mononucleosis,[1] and it has been associated with two geographically restricted malignancies, Burkitt's lymphoma and nasopharyngeal carcinoma.[2–5] Therefore, it is important to develop an animal model of EBV-induced tumor to facilitate studies on the relationship between EBV and human malignancies and to explore the molecular mechanism of EBV oncogenicity.

EBV specifically infects human and a few primates. So it has been very difficult to find a suitable animal model until the development of the C.B.-17 scid/scid mutant strain of mouse (hereafter referred to as the SCID (severe combined immunodeficiency) mouse). SCID mice exhibit a severe combined immunodeficiency characterized by the congenital absence of mature B and T lymphocytes because of gene mutation; indeed, the mutation is thought to affect a component of the recombinase enzyme system involved in *Ig* and *TCR* gene rearrangements. Therefore, SCID mouse can accept xenografts such as human lymphocytes. Our group and other researchers have successfully established an experimental model of EBV-induced lymphomas in human peripheral blood lymphocyte (hu-PBL)/SCID chimeras.[6–8] However, some of the mice died of acute graft-versus-host disease (GVHD) within 3 weeks after hu-PBLs were transplanted, because of heterogeneous antigens. Clinically, immunosuppressive drugs, including methotrexate, cyclosporine A (CSA), rapamycin (RAP), FK506, etc., are used for the prevention and treatment of graft rejection, GVHD and autoimmune disorders.[9–12] CSA-based post-graft immunosuppression has been crucial in achieving improved survival in patients given organ allografts.[13, 14] For this reason, we tried to apply CSA to inhibit graft-versus-host response in hu-PBL/SCID chimeras.

In addition, it is of crucial significance to find non-invasive techniques for early detection of acute rejection in hu-PBL/SCID chimeras. Since acute rejection leads to a dramatic activation of lymphocytes and macrophages that locally release cytokines and other inflammatory mediators, it might be possible to measure such molecules or their soluble receptors in biological fluids. Binding of host antigens to human T-cell receptors of xenografts induces interleukin (IL) 2, a powerful messenger for subsequent cellular immune responses. Once secreted, IL-2 promotes the expression of its high-affinity heterodimeric receptor (IL-2R) on the surface of target immune cells and the release of a 35- to 45-kDa, soluble, extracellular portion of the receptor (sIL-2R).[15] The latter can be detected in serum and urine by means of immunochemical assays. Serum concentrations of the 45-kDa α-chain soluble form can be used as a surrogate marker for T-cell activation and IL-2R expression.[16] Higher levels of sIL2-R have been reported in kidney and liver allograft recipients undergoing transplant rejection[17, 18] and in patients with autoimmune diseases.[19]

Here we report the effect of CSA on GVHD in hu-PBL/SCID chimeras and we also show that measurement of the serum concentration of human sIL-2R in the mice is useful to detect the appearance of GVHD and to verify the effect of CSA on GVHD.

Materials and Methods

PBL isolation and transfer to SCID mice. Human peripheral blood was obtained from 20 healthy blood volunteer donors (200–300 ml per person). Serum was separated from 2 ml of whole blood of each donor at the same time. The EBV immune status of blood donors was assessed with a commercial assay for serum antibody against EBV capsid antigen. PBLs were isolated

E-mail: gan998@yahoo.com

by Ficoll-Hypaque gradient centrifugation, washed 4 times with RPMI-1640 medium free of bovine serum and then counted. SCID mice were purchased from the Laboratory Animal Center of Chinese Science Academy (Beijing), and maintained in our facilities under special pathogen-free conditions. Groups of 4- to 6-week-old mice of both sexes were inoculated with intraperitoneal (i.p) 8 to 10×10^7/ml PBLs derived from one donor for each mouse. After 1 week, mice with hu-PBL engraftment from health IgG/VCA-negative donors were injected i.p. with 0.4 ml of EBV-containing supernatant from B95-8 cell suspension culture per mouse (active infection); the infectious EBV titer was 10^{-3}. Hu-PBL/SCID mice were considered latently infected with EBV when engrafted with PBL from EBV-seropositive donors; these mice were not injected with EBV derived from B95-8 supernatant (latent infection). The mice with only hu-PBL engraftment from health EBV seronegative donors were used as the control group for tumor induction in this experiment. The SCID mice were divided into four groups (Table 1).

CSA injection. Cyclosporine A (purchased from Sandoz Co., Novertis, Switzerland) was diluted to 1 mg/ml with 0.9% NaCl. In the present experiment, CSA was injected i.p into SCID mice after engraftment with hu-PBL from EBV-seronegative donors (see Table 1, active EBV infection plus CSA group) at 10 mg/kg/day on the first 2 days, and then 15 mg/kg every other day for 3 weeks.

Examination of neoplasms in SCID mice. The animals were observed every day for signs of illness; when they became sick, they were killed by exposure to excess ethyl-ether and autopsied. In other SCID mice, follow-up was extended to 135 days. Tumors were cut into 2 parts: one was immediately frozen at −80°C for DNA analysis; the other part was fixed in 10% neutralized formalin, embedded in paraffin and sectioned at 4 μm for histopathologic observation.

ELISA for sIL-2R. The mice were bled from a tail vein at days 3, 7, 15, 22, and 33 post PBL engraftment in the active EBV infection plus CSA group and in the active EBV infection group without CSA administration; serum samples were stored at −80°C until use. The concentrations of sIL-2R were assessed using a commercial ELISA kit, which is a sandwich enzyme immunoassay for the detection of released sIL-2R in serum.[20, 21] Microtiter wells were purchased with anti-IL-2R monoclonal coating antibody, as well as soluble IL-2R as a standard. Aliquots of 50 μl of mouse sera and diluted standard samples were added to wells, and the plates were incubated at 43°C for 30 min. After several washings, an enzyme-conjugated anti-IL-2R monoclonal antibody against the second epitope on IL-2R was added to complete the sandwich. Subsequently, the wells were washed to remove unbound components and substrate solution was added. The reaction was halted by adding stopping solution, and absorbance was read at 490 nm in a plate reader. The sIL-2R values of standard serum samples supplied with the test kit were recorded as unit/ml±SD. Results are expressed as mean±SD, and the significance of differences between mean values was analyzed by means of Student's paired *t* test. Differences were considered significant if $P\leq0.05$.

Immunohistochemistry. Immunohistochemical staining using anti-human LCA (CD45), PS1 (CD3), L26 (CD20), UCHL-1 (CD45RO) (purchased from Maxin Co., San Francisco, LA), and anti-LMP1 (purchased from Dako Co., Kyoto) were performed according to the manufacturer's protocol. Briefly, endogenous peroxidase was quenched with 0.3% hydrogen peroxide, non-specific binding was blocked with normal non-immune serum, and tissue slides were incubated with each specific antibody at 4°C overnight. Bound antibody was detected with biotin-conjugated secondary antibody followed by streptavidin-peroxidase and diaminobenzidine (DAB) color reagent. Hematoxylin counter-stain was employed to enhance the visualization of tissue architecture and cytological morphology.

Transmission electron microscopy. Tumor tissues were fixed in 2.5% glutaraldehyde, refixed with 1% osmic acid, dehydrated with an acetone series, embedded in Epon812 and cut into ultrathin sections with LKB-III type ultramicrotome. The sections were double-stained with dioxygen uranium acetate and lead citrate, then observed under the transmission electron microscope to search for EBV particles.

***In situ* hybridization (ISH).** *In situ* hybridization for Epstein-Barr virus (EBV)-encoded small RNA-1 (EBER1) is currently the most dependable method to detect EBV in cells. The oligonucleotide sequence of the synthetic EBER1 probe[6] was: 5′-CTC CTC CCT AGC AAA ACC CTC AGG ACG GCG-3′. The probes were end-labeled with digoxigenin by tailing with terminal transferase. The labeling reaction was set up according to the manufacturer's protocol (Boehringer Mannheim Co., Ingelheim, Germany). *In situ* hybridization using EBER1 probe was carried out as follows. Briefly, the slides were pretreated with 2% APES, and 4-μm tissue slices of the induced tumors were heated for 1 h at 70°C, then dewaxed in xylene. The tissue slices were digested with 0.5% μg/ml proteinase K for 10 min at 37°C, and then washed. The labeled probes were diluted to a concentration of 100 ng/ml in hybridization medium (25% deionized formamide, 4× SSC (sodium citrate, sodium chloride), 50 mmol/liter NaH_2PO_4/Na_2HPO_4,1 mmol/liter EDTA, 5× Denhart's, 1 mg/ml ssDNA), and spotted onto the tissue slices, which were covered with a coverslip. The DNA probe and target RNA in tissue slices were simultaneously denatured at 70°C for 8 min. Then the sections were hybridized at 37°C for 4 h or overnight. Non-specifically bound or unbound probe was removed by two post-hybridization washes of 10 min in 2× SSC and 10 min in 0.1× SSC at room temperature. The slices were blocked with 2% normal goat serum at room temperature for 20 min, followed by incubation with anti-digoxigenin antibody at 37°C for 30 min, then washed 3 times. NBT/NCIP was used as the chromogen. Counter-staining was done with nuclear fast red.

Alu-PCR. DNA was extracted with phenol-chloroform from frozen biopsy material of the induced tumors. Primers (sense 5′-CAC CTG TAA TCC CAG CAG TTT-3′; anti-sense 5′-CGC GAT CTC GGC TCA CTG CA-3′)[22] were used in the PCR to amplify a 221-bp sequence for human-specific Alu. PCR was performed under the following conditions: 95°C predenaturation for 5 min, and then 30 cycles of denaturation at 94°C for 1 min, annealing at 57°C for 1 min and extension at 72°C for 1 min.

Results

Occurrence of GVHD in hu-PBL/SCID mice. None of 14 hu-PBL/SCID mice died of GVHD in the active EBV infection group

Table 1. Experimental groups of SCID mice

Experimental group	Hu-PBL inoculation	Status of EBV immune	Active EBV injection	CSA administration	Number of mice
Active infection	+	−	+	−	23
Active infection plus CSA	+	−	+	+	14
Latent infection	+	+	−	−	18
Control group	+	−	−	−	9

with CSA administration, while 17 mice died of GVHD in other three groups (see Table 2). The survival time ranged from 12 days to 43 days after hu-PBL transplantation and the median time was 17 days. The mortality in each group is given in Table 2. The death rate in the CSA group was significantly different from those in other groups ($P<0.01$). The results showed that CSA could effectively inhibit the incidence of GVHD in hu-PBL/SCID chimeras. In macroscopic examination, many sporadic, sesamoid lesions with gray-white color could be found on the surface of and inside the liver in these 17 mice. Microscopically, of the liver contained many sporadic coagulative necrotic lesions (Fig. 1), which were infiltrated with many lymphocytes and monocytes. Sinus hepaticua was dilated and congested. There were also some necrotic foci, lymphocyte and monocyte infiltration and hyaline thrombi in kidneys and lungs in SCID mice that had died of GVHD.

Assay of human sIL-2R in serum of hu-PBL/SCID mice. We measured serum concentrations of human sIL-2R in the active EBV infection plus CSA group and in the active EBV infection group without CSA administration. The sIL-2R levels in sera of hu-PBL/SCID mice were stable in the active EBV infection plus CSA group on days 3, 7, 15, 22 and 33 after hu-PBL transplantation. In contrast, the sIL-2R values increased considerably in a short time and peaked on day 22 in the active EBV infection group without CSA. There were significant differences of sIL-2R concentration between day 3 and day 15, and between day 3 and day 22 ($P<0.05$) in the no CSA group. Moreover, three mice in that group died of GVHD on days 12, 14 and 16, respectively. On the other hand, serum sIL-2R levels were significantly higher in the active EBV infection group without CSA administration than in the active infection plus CSA group at day 15 and day 22 after hu-PBL engraftment (both $P<0.05$) (Fig. 2).

Generation of EBV-induced tumors. Thirty-two of the 43 surviving hu-PBL/SCID mice with EBV infection developed tumors in the peritoneal cavity and/or mediastinum. The survival time of mice with induced tumors varied from 31 days to 137 days after hu-PBL engraftment, and the median survival time of tumor-bearing mice was 60 days. The incidence of tumors was 68.75% in the active EBV infection group without CSA administration, 71.43% in the active EBV infection plus CSA group, and 76.92% in the latent EBV infection group (Table 3). There was no significant difference of tumor incidence between the two active EBV infection groups with CSA and without CSA administration ($P>0.05$). Tumors were solid, malacoid, irregular nodules (Fig. 3) without an envelope, adhering to surrounding organs and tissues. Their incisional side views were gray-white or gray-red, and gray-yellow necrotic loci could often be seen in the center of some bigger tumors. Morphologically, neoplasms of all cases exhibited a diffuse infiltrative pattern of tumor growth. Tumors invaded the liver, kidney, pancreas, lungs and musculi of the thoracic and abdominal regions. The neoplastic cells were polymorphic, mixed with large cleaved and non-cleaved, plasmacytoid or immunoblastic lymphocytes (Fig. 3), containing large, round to slightly irregular nuclei and abundant cytoplasm. Immunohistochemical staining showed that LCA (leukocyte common antigen) was positive, B-cell marker (CD20) was positive, and T-cell markers (CD3 and CD45RO) were negative in all tumors. From their morphological and immunohistochemical features, those tumors can be diagnosed as human B-cell lymphomas. Alu-PCR showed that all of tumor tissues contained 221-bp Alu sequence. This confirmed that induced tumors in hu-PBL/SCID chimeras were derived from human, but not from mouse.

There were EBV particles in nuclei of tumor cells observed by transmission electron microscopy. The central nucleic acid of the virus is surrounded by an icosahedral capsid measuring 100–140 nm in diameter (Fig. 4). The EBV expression product LMP-1 could be detected in some tumor cells by immunohistochemistry. The *in situ* hybridization signal of EBER1 was very intense with a diffuse pattern of staining confined to the nucleus (sparing the nucleus) in all cases. Notably, almost all morphologically malignant cells exhibited positive signals with the EBER1 probe, while the normal host tissue adjacent to tumors showed negative (Fig. 5).

Discussion

The pathogenesis of GVHD involves immunocytes of the graft inducing an immune response to tissue antigens of the host. GVHD is usually found in bone marrow transplantation (BMT), and moreover acute GVHD always appears 10–50 days after BMT.[23, 24] SCID mouse congenitally lacks both T and B cells because of gene mutation. When SCID mice are inoculated with sufficient human lymphocytes, GVHD may occur in the hu-PBL/SCID mice owing to interspecies heteroantigen differences. In the present experiments, the survival time of the mice that died of GVHD was 12–43 days, and this is consistent with the time when acute GVHD appears in patients. Further, typical lesions of rejection reaction were observed in the mice: coagu-

Table 2. Inhibitory effect of CSA on GVHD occurrence in hu-PBL/SCID mice

Experimental group	Number of mice engrafted with hu-PBLs	Number of mice died of GVHD	Mortality (%)
Active infection[a]	23	7	30.43
Active infection plus CSA[b]	14	0	0
Latent infection[c]	18	5	27.78
Control group[d]	9	5	55.56

b vs. a, c, d group: exact probabilities $P=0.004$.

Table 3. Tumor generation of hu-PBL/SCID mice induced by EBV

Experimental group	Number of surviving mice	Number of mice with tumors	Tumor-induction rate (%)
Active infection[a]	16	11	68.75
Active infection plus CSA[b]	14	11	71.43
Latent infection[c]	13	10	76.92
Control group[d]	4	0	0

d vs. a, b, c group: exact probabilities $P=0.0136$. b vs. a group: $P>0.05$. b vs. c group: $P>0.05$.

lative necrotic lesions in liver, kidneys and lungs, thrombosis in small blood vessels, lymphocyte infiltration of solid organs in the host, etc.

Clinical and experimental researches have proved that T-cells are the main responding cells that cause GVHD.[25] Selective depletion of donor T-cells has proved to be effective in preventing acute GVHD.[26, 27] CSA inhibits Th cells, but has little effect on Ts, B and macrophages.[28, 29] Our results showed CSA could strikingly inhibit GVHR in hu-PBL/SCID mice, allowing us to establish a stable lymphoma model. Of 43 surviving mice that escaped GVHD, 32 developed tumors, i.e., the overall rate of tumor induction was 74.42% (32/43 mice). There was no significant difference between the active EBV infection groups with CSA and without CSA administration, which indicated that CSA did not influence the development of EBV-induced tumors. Seventeen mice in the three groups without CSA administration died of GVHD. Mortalities were 55.56% (5/9), 30.43% (7/23), and 27.78% (5/18), respectively. Since SCID mice are expensive, the use of CSA to prevent GVHD after hu-PBL transplantation will be highly beneficial. Interestingly, no mouse died in the active EBV infection group with CSA administration.

In the present experiment, we observed the development of EBV-related lymphoma in SCID mice engrafted with hu-PBLs. The tumor is solid, aggressive and fatal, and belongs to the category of highly malignant non-Hodgkin's lymphoma (NHL) in terms of histopathology. Both *Alu*-gene detection and monoclonal antibody examination have shown that the induced tumors were derived from human B-lymphocytes. The tumor cells contained EBV small RNA molecule (EBER-1) and protein expression (LMP1), and furthermore, EBV particles were present in the nuclei of tumor cells. This EBV-induced tumor model has many advantages as follows: (a) The normal human cells come from healthy adult PBLs, so the experimental samples are easy to collect. (b) Oncogenic EBV is a standard virus strain isolated from B95-8 cell line, and it is extensively used by researchers. (c) SCID mice are readily available, in contrast to primates, although they must be maintained in a specific pathogen-free (SPF) environment. (d) Tumor induction is

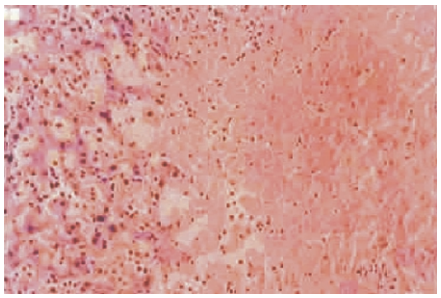

Fig. 1. Coagulative necrotic lesion of GVHD in hu-PBL/SCID mice. Hepatocyte focal necrosis (right) in mouse liver (HE stain ×200).

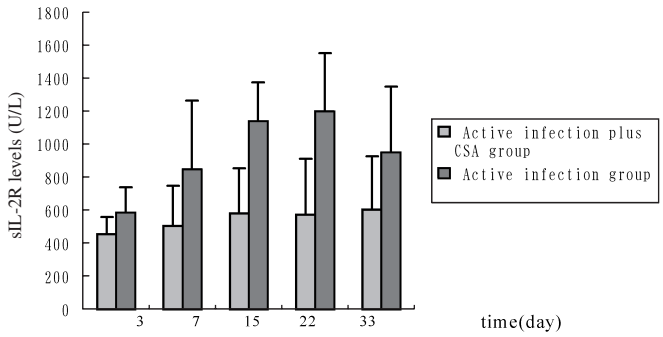

Fig. 2. Serum levels of sIL-2R at different time points after hu-PBL transplantation. The sIL-2R values were stable in hu-PBL/SCID mice of the active EBV infection plus CSA group on days 3, 7, 15, 22 and 33, whereas the sIL-2R values increased dramatically and reached a peak on day 22 in the active EBV infection group without CSA.

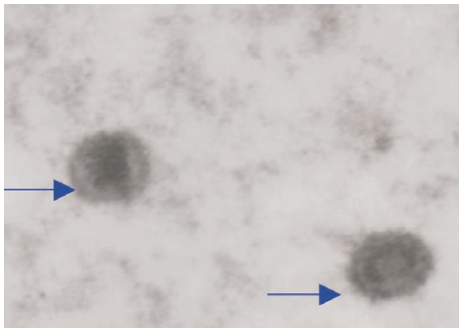

Fig. 4. Electron micrograph of thin section of tumor tissue from the body of a SCID mouse. Arrows indicate immature EBV particles in the nucleus of a tumor cell (×64,000).

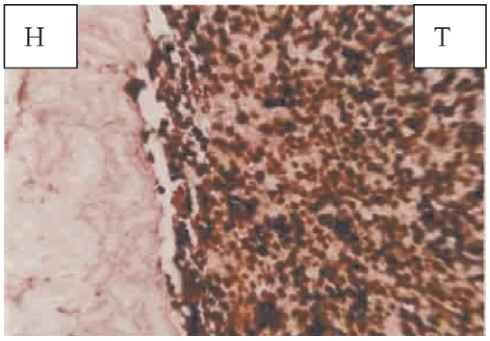

Fig. 5. Expression of small RNA molecules, EBER1, was seen in almost all nuclei (T) of EBV-induced tumors, whereas renal tissue of SCID mice was negative (H).

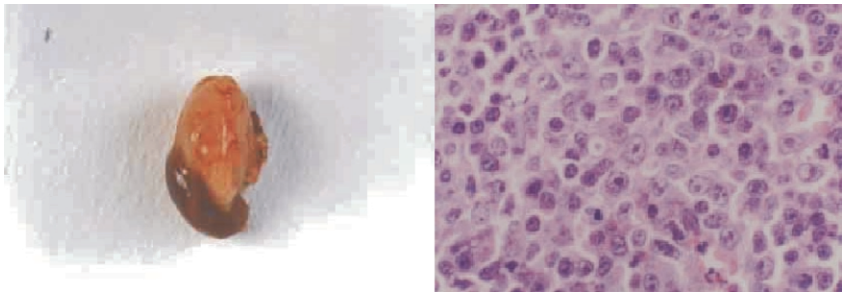

Fig. 3. Fresh tumor tissue showed gray-white and gray-red node, size 17×11×8 mm, adhering to mouse kidney (left). Microscopically, tumor cells exhibited human diffuse large cell lymphoma, with differentiation of immunoblastic and plasmacytoid lymphocytes (right). HE stain ×400.

straightforward, and the experimental cycle lasts only 2 months, while the incidence of EBV-associated tumors in surviving mice can reach 74.42%. (e) The solid induced tumor shows histopathology, morphology and growth behavior in line with those of human malignant lymphomas. (f) EB viruses are widespread in the tumor cells, and thus should be the predominant factor in tumor induction. This model can provide evidence for the causal relationship between EBV infection and tumorigenesis in human normal cells. It should also be suitable for studies on the molecular mechanisms of EBV-related tumors.

IL-2 is a lymphokine which is synthesized by activated T lymphocytes, and exerts its biological effect by binding to high-affinity IL-2R on the surface of activated lymphocytes.[15] sIL-2R is a fragment released from surface-bound IL-2R. It has been reported that the application of CSA not only inhibits GVHR clinically, but also decreases the production of sIL-2R.[9, 30, 31] Mathias *et al*.[32] measured serial sIL-2R concentrations weekly for 4 weeks in 43 patients after allogeneic BMT to determine if the sIL-2R concentration is a useful marker to help establish a diagnosis of acute GVHD. They found that 23 patients developed acute GVHD and there was a significant association between a clinical diagnosis of acute GVHD and an increase in the sIL-2R concentration. In the present study, we examined human sIL-2R levels in the serum of hu-PBL/SCID chimeras. Over the first 33 days after hu-PBL transplantation, serum level of human sIL-2R in hu-PBL/SCID chimeras were stable in the active EBV infection plus CSA group, while sIL-2R concentration gradually increased in the sera of active EBV infection mice without CSA administration and peaked at 22 days. Thus, sIL-2R could be a valuable indicator of both the change in xenoantigen-induced immune response and the effectiveness of CSA immunosuppressive treatment. We therefore believe that CSA will become a valuable adjunct for construction of human PBL/SCID chimeras to establish a stable tumor model associated with EBV in SCID mice.

The authors would like to thank Prof. Kaitai Yao for his advice. This work was supported by the National Nature Scientific Fund of China (No. 39070921) and the Key Fund of Scientific Research on Common Malignant Neoplasms of Health Department in Hunan Province of China (No. 9751).

1. Papesch M, Watkins R. Epstein-Barr virus infectious mononucleosis. *Clin Otolaryngol* 2001; **26**: 3–8.
2. Chan KC, Zhang J, Chan AT, Lei KI, Leung SF, Chan LY, Chow KC, Lo YM. Molecular characterization of circulating EBV DNA in the plasma of nasopharyngeal carcinoma and lymphoma patients. *Cancer Res* 2003; **63**: 2028–32.
3. Westphal EM, Mauser A, Swenson J, Davis MG, Talarico CL, Kenney SC. Induction of lytic Epstein-Barr virus (EBV) infection in EBV-associated malignancies. *Cancer Res* 1999; **59**: 1485–91.
4. Henry S, Sacaze C, Berrajah L, Karray H, Drira M, Hammami A, Icart J, Mariame B. In nasopharyngeal carcinoma-bearing patients, tumors and lymphocytes are infected by different Epstein-Barr virus strains. *Int J Cancer* 2001; **91**: 698–704.
5. Baran-Marszak F, Fagard R, Girard B, Camilleri-Broet S, Zeng F, Lenoir GM, Raphael M, Feuillard J. Gene array identification of Epstein Barr virus-regulated cellular genes in EBV-converted Burkitt lymphoma cell lines. *Lab Invest* 2002; **82**: 1463–79.
6. Gan R, Lan K, Yin Z, Wang L, Xiu L, Yao K. Development of human B-cell lymphomas induced by Epstein-Barr virus in SCID mouse. *Chin J Clin Oncol* 2002; **29**: 733–8.
7. Funakoshi S, Beckwith M, Fanslow W, Longo DL, Murphy WJ. Epstein-Barr virus-induced human B-cell lymphoma arising in Hu-PBL/SCID chimeric mice: characterization and the role of CD40 stimulation in their treatment and prevention. *Pathobiology* 1995; **63**: 133–42.
8. Fuzzati-Armentero MT, Duchosal MA. Hu-PBL-SCID mice: an *in vivo* model of Epstein-Barr virus-dependent lymphoproliferative disease. *Histol Histopathol* 1998; **13**: 155–68.
9. Strauss G, Osen W, Debatin KM. Induction of apoptosis and modulation of activation and effector function in T cells by immunosuppressive drugs. *Clin Exp Immunol* 2002; **128**: 255–66.
10. Asano M, Gundry SR, Izutani H, Cannarella SN, Fagoaga O, Bailey LL. Baboons undergoing orthotopic concordant cardiac xenotransplantation surviving more than 300 days: effect of immunosuppressive regimen. *J Thorac Cardiovasc Surg* 2003; **125**: 60–9.
11. Saunders RN, Bicknell GR, Nicholson ML. The impact of cyclosporine dose reduction with or without the addition of rapamycin on functional, molecular, and histological markers of chronic allograft nephropathy. *Transplantation* 2003; **75**: 772–80.
12. Sokol DK, Molleston JP, Filo RS, Van Valer J, Edwards-Brown M. Tacrolimus (FK506)-induced mutism after liver transplant. *Pediatr Neurol* 2003; **28**: 156–8.
13. Arranz R, Conde E, Rodriguez-Salvanes F, Pajuelo FJ, Cabrera R, Sanz MA, Petit J, Bueno J, Maldonado J, Odriozola J, Conde JG, Brunet S, Carreras E, Iriondo A, Fernandez-Ranada JM, Marin P. CSA-based post-graft immunosuppression: the main factor for improving outcome of allograft patients with acquired aplastic anemia. *Bone Marrow Transplant* 2002; **29**: 205–11.
14. Gonwa TA, Hricik DE, Brinker K, Grinyo JM, Schena FP. Improved renal function in sirolimus-treated renal transplant patients after early cyclosporine elimination. *Transplantation* 2002; **74**: 1560–7.
15. Osorio LM, Rottenberg M, Jondal M, Chow SC. Simultaneous cross-linking of CD6 and CD28 induced cell proliferation in resting T cells. *Immunology* 1998; **93**: 358–65.
16. Morris JC, Waldmann TA. Advances in interleukin 2 receptor targeted treatment. *Ann Rheum Dis* 2000; **59** Suppl 1: i109–14.
17. Casiraghi F, Ruggenenti P, Noris M, Locatelli G, Perico N, Perna A, Remuzzi G. Sequential monitoring of urine-soluble interleukin 2 receptor and interleukin 6 predicts acute rejection of human renal allografts before clinical or laboratory signs of renal dysfunction. *Transplantation* 1997; **63**: 1508–14.
18. Lun A, Cho MY, Muller C, Staffa G, Bechstein WO, Radke C, Neuhaus P, Renz H. Diagnostic value of peripheral blood T-cell activation and soluble IL-2 receptor for acute rejection in liver transplantation. *Clin Chim Acta* 2002; **320**: 69–78.
19. Dejica D. Serum soluble IL-2 receptor as a marker of lymphocyte activation in some autoimmune diseases. *Roum Arch Microbiol Immunol* 2001; **60**: 183–201.
20. Papadaki HA, Coulocheri S, Eliopoulos GD. Patients with chronic idiopathic neutropenia of adults have increased serum concentrations of inflammatory cytokines and chemokines. *Am J Hematol* 2000; **65**: 271–7.
21. Porcel JM, Gazquez I, Vives M, Perez B, Rubio M, Rivas MC. Diagnosis of tuberculous pleuritis by the measurement of soluble interleukin 2 receptor in pleural fluid. *Int J Tuberc Lung Dis* 2000; **4**: 975–9.
22. Fukuchi Y, Miyakawa Y, Kizaki M, Umezawa A, Shimamura K, Kobayashi K, Kuramochi T, Hata J, Ikeda Y, Tamaoki N, Nomura T, Ueyama Y, Ito M. Human acute myelo-blastic leukemia-ascites model using the human GM-CSF- and IL-3-releasing transgenic SCID mice. *Ann Hematol* 1999; **78**: 223–31.
23. Fauser AA, Basara N, Blau IW, Kiehl MG. A comparative study of peripheral blood stem cell vs bone marrow transplantation from unrelated donors (MUD): a single center study. *Bone Marrow Transplant* 2000; **25** Suppl 2: S27–31.
24. Ji S, Chen H, Wang H, Ma J, Pan S, Xue M, Zhu L, Liu J, Xiao M, Zhou L. Low incidence of severe aGVHD and accelerating hemopoietic reconstitution in allo-BMT using lenograstim stimulated BM cells. *Chin Med J* 2001; **114**: 191–5.
25. Kroger N, Einsele H, Wolff D, Casper J, Freund M, Derigs G, Wandt H, Schafer-Eckart K, Wittkowsky G, Schmitz N, Kruger W, Zabelina T, Renges H, Ayuk F, Krull A, Zander A. Myeloablative intensified conditioning regimen with *in vivo* T-cell depletion (ATG) followed by allografting in patients with advanced multiple myeloma: a phase I/II study of the German Study-group Multiple Myeloma (DSMM). *Bone Marrow Transplant* 2003; **31**: 973–9.
26. Van Dijk AM, Kessler FL, Stadhouders-Keet SA, Verdonck LF, de Gast GC, Otten HG. Selective depletion of major and minor histocompatibility antigen reactive T cells: towards prevention of acute graft-versus-host disease. *Br J Haematol* 1999; **107**: 169–75.
27. Simpson D. T-cell depleting antibodies: new hope for induction of allograft tolerance in bone marrow transplantation. *Bio Drugs* 2003; **17**: 147–54.
28. Shaw KT, Ho AM, Raghavan A, Kim J, Jain J, Park J, Sharma S, Rao A, Hogan PG. Immunosuppressive drugs prevent a rapid dephosphorylation of transcription factor NFAT1 in stimulated immune cells. *Proc Natl Acad Sci USA* 1995; **92**: 11205–9.
29. Krook H, Wennberg L, Hagberg A, Song Z, Groth CG, Korsgren O. Immunosuppressive drugs in islet xenotransplantation: a tool for gaining further

insights in the mechanisms of the rejection process. *Transplantation* 2002; **74**: 1084–9.
30. Miyamono T, Akashi K, Hayashi S, Gondo H, Murakawa M, Tanimoto K, Harada M, Niho Y. Serum concentration of the soluble interleukin-2 receptor for monitoring acute graft-versus-host disease. *Bone Marrow Transplant* 1996; **17**: 185–90.
31. Economidou J, Barkis J, Demetriou Z, Avgerinou G, Psarra K, Degiannis D, Vareltzidis A, Katsambas A. Effects of cyclosporin A on immune activation markers in patients with active psoriasis. *Dermatology* 1999; **199**: 144–8.
32. Mathias C, Mick R, Grupp S, Duffy K, Harris F, Laport G, Stadtmauer E, Luger S, Schuster S, Wasik MA, Porter DL. Soluble interleukin-2 receptor concentration as a biochemical indicator for acute graft-versus-host disease after allogeneic bone marrow transplantation. *J Hematother Stem Cell Res* 2000; **9**: 393–400.